Coexistence of ferromagnetic and spin-glass phenomena in $La_{1-x}Ca_xMnO_3$ ($0 \leq x \leq 0.4$)

2000 J. Phys.: Condens. Matter 12 5751

(http://iopscience.iop.org/0953-8984/12/26/321)

J. Phys.: Condens. Matter **12** (2000) 5751–5764. Printed in the UK PII: S0953-8984(00)13028-0

Coexistence of ferromagnetic and spin-glass phenomena in $La_{1-x}Ca_xMnO_3$ ($0 \leqslant x \leqslant 0.4$)

R Laiho†, K G Lisunov‡, E Lähderanta†, P Petrenko‡, J Salminen†, V N Stamov‡ and V S Zakhvalinskii‡

† Wihuri Physical Laboratory, Department of Physics, University of Turku, FIN-10014 Turku, Finland

‡ Institute of Applied Physics, Academiei Street 5, MD-2028 Kishinev, Moldova

Received 3 April 2000

Abstract. Low-field magnetic properties of ceramic $La_{1-x}Ca_xMnO_3$ ($0 \leqslant x \leqslant 0.4$) are investigated between $T = 5$ and 310 K. The paramagnetic–ferromagnetic transition is observed in all the samples. The dependence of the Curie temperature, T_C, on x is described within a model of spin polarons associated with electronic localization. Critical behaviour of the susceptibility $\chi^{-1}(T) \sim (T - T_C)^{\gamma}$ is observed for $T > T_C$, with the critical exponents $\gamma = 1.20 \pm 0.05$ and $\gamma^* = 1.64 \pm 0.06$ below and above the composition $x \approx 0.18$ corresponding to the Mn^{4+} ion concentration $c \approx 0.23$, respectively. For the compound with $x = 0.3$ no temperature hysteresis of the resistivity is observed in magnetic fields between 0 and 8 T. In all the samples the field-cooled and zero-field-cooled magnetizations deviate below T_C, the difference being approximately equal to the thermoremanent magnetization (TRM). Long-time relaxation of TRM in LCMO is observed for time scales up to 10^4 s. The relaxation rate reaches a maximum near a wait time $t_W \sim 10^3$ s. The time dependence of TRM can be described with a stretched exponential law, as in spin or cluster glasses in conditions where the observation time is comparable with t_W.

1. Introduction

The mixed-valence material $La_{1-x}Ca_xMnO_3$, briefly LCMO, has received much attention due to a very large ('colossal') negative magnetoresistance around the paramagnetic (PM) to ferromagnetic (FM) transition temperature, T_C, of the compound [1]. Both magnetic and transport properties of LCMO and related compounds (manganite and cobaltite perovskites) are determined to a great degree by the ratio of the Mn^{4+} and Mn^{3+} ion concentrations, c. The value of c can be varied by hole doping, achieved by substitution of a divalent alkaline element such as Ca^{2+} for La^{3+} [2], by formation of vacancies in the metal sublattice [3, 4] or by deviations from the exact oxygen stoichiometry [5]. The variety of electronic and magnetic properties of LCMO involves an antiferromagnetic (AFM) insulating state below the Néel temperature T_N for $0 \leqslant c < 0.15$–0.20, the FM metallic phase for 0.15–$0.20 < c < 0.5$ and $T < T_C$ [2, 6], charge ordering near $c \approx 0.5$ [7, 8] and canted spin orientation below a temperature $T_1 < T_C$ or T_N [9, 10]. Basically, the magnetic state of LCMO is determined by competition between the Mn^{3+}–Mn^{3+} superexchange (SE) interaction, leading to the AFM ordering and the double-exchange (DE) mechanism aligning the Mn^{3+}–Mn^{4+} spins ferromagnetically by electron transfer via O^{2-} ions [9, 10]. On the other hand, the simple picture including only SE and DE interactions has been found to be incomplete due to omission of the electron–lattice interaction and association of the Jahn–Teller effect (JT) was suggested [11]. As a consequence

0953-8984/00/265751+14$30.00

of the JT effect theoretical attempts were made to incorporate lattice polarons in perovskite manganites [12, 13]. Additionally, the importance of spin polarons associated with electronic localization due to magnetic disorder and electron–electron interaction in these materials has been demonstrated [14]. Neutron-scattering experiments have established the existence of droplets with magnetic coupling different from the matrix in the FM phase of LCMO [15] and evidence of small FM clusters/polarons present within the PM phase of $La_{0.67}Sr_{0.33}MnO_3$ [16] and in $La_{0.75}Ca_{0.2}Mn(Co)O_3$ [17] has been obtained. In $La_{0.8}Ca_{0.2}Mn(Co)O_3$ it was found that upon approaching T_C from the low temperature side the FM phase breaks down to small superparamagnetic clusters with size of ∼5–10 nm [18].

The presence of different magnetic sublattices with disorder and competing SE–DE interactions, on one hand, and the phase separation or existence of hole-rich droplets (magnetic polarons or clusters) with properties and interactions differing from the host material, on the other hand, can give rise to frustrated spin-glass (SG), cluster-glass (CG) or re-entrant FM states in addition to the ordered magnetic phases mentioned above. Irreversible magnetization inherent to a frustrated magnetic state has actually been observed in low fields in different manganite and cobaltite perovskites [4, 5, 19–22]. In this paper we present low-field dc magnetization results, including time-dependent effects, which give evidence for coexistence of FM and SG-like phases in LCMO.

2. Experimental methods

The LCMO samples ($0 \leqslant x \leqslant 1$) were synthesized with a standard ceramic technique (see e.g. [6]) by mixing stoichiometric proportions of La_2O_3, $CaCO_3$ and MnO_2 and heating in air at 1320 °C at first for 15 h, then for 5 h, and at 1375 °C for 22 h with intermediate grindings (A samples). Some of the specimens with $0 \leqslant x \leqslant 0.4$ was subjected to an additional heat treatment at 1520 °C for 13 h (B samples). According to x-ray diffraction data all samples were of single phase, having the undistorted cubic structure (space group P_m3_m) [23]. The linear dependence of the lattice parameter on composition, $a(x) = a_0 - a_1x$ with $a_0 = 7.846 \pm 0.005$ Å and $a_1 = 0.399 \pm 0.009$ Å was observed for $0.15 \leqslant x \leqslant 1$. Our values of a are close to those quoted for cubic LCMO with $0 \leqslant x \leqslant 0.5$ [2].

DC magnetic measurements were made with a SQUID magnetometer using A and B samples with $x = 0$, 0.05, 0.15, 0.2, 0.3 and 0.4. The B samples are denoted below by 1, 2, ... 6, (table 1), and the A samples have the same numbers with asterisks (table 2). The temperature dependence of the magnetization, $M(T)$, was measured after cooling the sample from 310 K to 5 K in zero ($B < 0.1$ G) field (ZFC) or in the field of 2 G (FC). The temperature dependence of the thermoremanent magnetization (TRM) was measured after cooling the samples in the field of 2 G from room temperature down to 5 K and then reducing the field to

Table 1. Composition (x) and concentration of Mn^{4+} (c) of the B samples.

Sample No	x	c
1	0.00	0.19
2	0.05	0.15
3	0.15	0.20
4	0.20	0.24
5	0.30	0.33
6	0.40	0.43

Table 2. Composition (x) and concentration of Mn^{4+} (c) of the A samples [23].

Sample No	x	c
1*	0.00	0.21
2*	0.05	0.18
3*	0.15	0.22
4*	0.20	0.26
5*	0.30	0.34
6*	0.40	0.43

zero. For investigation of the time decay of TRM the sample was first cooled in the field of 50 G from the room temperature down to the measuring temperature, T_m. After a wait time, $t_W \sim 10^3$ s, the field was abruptly reduced to zero and the decay of the TRM was recorded over a time period of about 10^4 s.

3. Results and discussion

3.1. Ferromagnetic transition in LCMO

As evident from figure 1, both the ZFC susceptibility, $\chi_{ZFC}(T)$, and FC susceptibility, $\chi_{FC}(T)$ ($\chi = M/B$) exhibit an FM transition at T_C depending on x (where T_C can be identified at an inflection point, common for both $\chi_{ZFC}(T)$ and $\chi_{FC}(T)$, or at a downward peak of their derivative over T [23]). Additionally, the plots of $\chi_{ZFC}(T)$ and $\chi_{FC}(T)$ diverge clearly below T_C. The magnetic irreversibility phenomena will be analysed in the next subsection. Here we discuss the dependence of T_C on composition and the critical behaviour of the magnetic susceptibility near T_C for our B samples. The corresponding data obtained previously for the A samples [23] will be displayed for completeness and comparison.

To analyse the dependence of T_C on x we apply the model of Varma [14], which treats the PM to FM transition in La manganites by considering the electron localization due to magnetic disorder and the electron–electron interactions. In this model the electrons are localized below the mobility threshold, inside a band with rectangular shape of the density of states and the bandwidth W. T_C satisfies the equation

$$T_C \cong 0.1 E^F_{coh}(c) \tag{1}$$

where $E^F_{coh}(c)$ is the electronic cohesive energy in the FM phase,

$$E^F_{coh}(c) = \frac{W}{2} c(1-c). \tag{2}$$

To determine the relation between c and x, we take into account a possibility that cation vacancies (with concentration δ) are generated during preparation of the samples, and that these vacancies can be occupied by Ca^{2+} ions. Each vacancy of the cation sublattice of LCMO yields three Mn^{4+} ions. Therefore, c is increased by one if one Ca^{2+} is substituted for La^{3+}, while c is decreased by two for occupation of a vacancy by Ca^{2+}. The concentration of Mn^{4+} at a given x can be written as $c(x) = c(0) + x_1 + x_2$, where $c(0) = 3\delta$, $x_1 = xP_1(x)$ is the concentration of Ca^{2+} ions substituted for La^{3+} and $x_2 = xP_2(x)$ is the concentration of Ca^{2+} ions which occupy the cation vacancies. Taking into account that the respective probabilities are $P_1(x) = x/(x+\delta)$ and $P_2(x) = \delta/(x+\delta)$, we obtain the concentration of the Mn^{4+} ions as

$$c(x) = \frac{x^2 + \delta x + 3\delta^2}{x+\delta}. \tag{3}$$

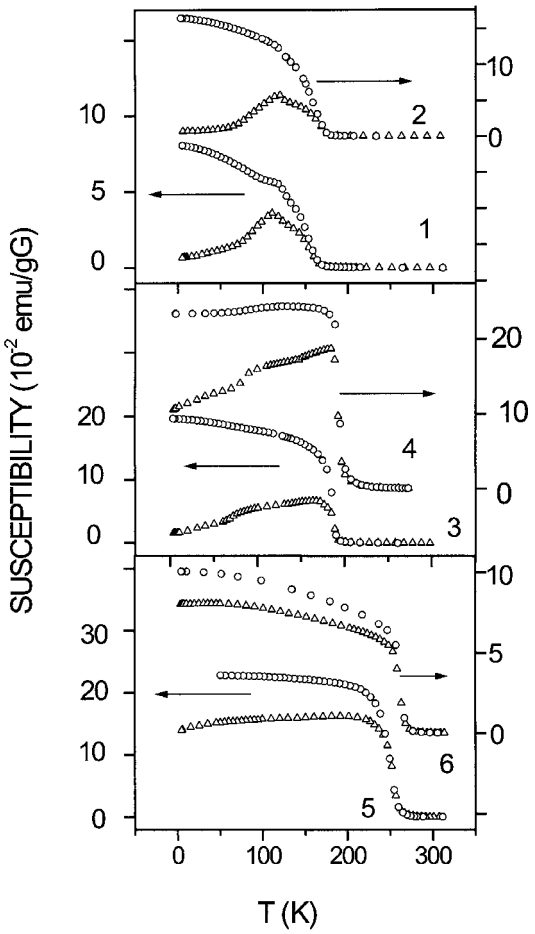

Figure 1. Temperature dependence of χ_{ZFC} (△) and χ_{FC} (○) for samples 1–6.

The experimental dependence of T_C on x is shown in figure 2(a) (closed triangles) together with the fit (solid line) calculated with equations (1)–(3), using W and δ as adjustable parameters. A reasonable agreement with the experimental data is obtained for $W = 1.88 \pm 0.06$ eV and $\delta = 0.062 \pm 0.006$. Note that δ should be sensitive to details of the preparation method and can vary randomly from sample to sample. However, as seen from figure 2(b) the dependence of c on x evaluated with equation (3) (solid line) is in the interval of $0.1 \leqslant x \leqslant 0.3$ very close to that obtained independently in [3] (open symbols). At low x the calculated dependence deviates distinctly from the concentration of Ca^{2+} (dashed line), agreeing well with the behaviour in [3]. The bandwidth W in LCMO is similar to that in $La_{1-x}Sr_xMnO_3$ ($W \approx 2.5$ eV) [14]. Finally, the values of c calculated for our samples with equation (3) are listed in table 1. All samples satisfy the conditions of the FM region of the magnetic phase diagram (see section 1).

The parameters of the A samples are shown in table 2 [23]. The values of T_C for the B samples are somewhat lower for low x and are practically the same for $x = 0.3$ and 0.4 as for the A samples [23]. The agreement of the dependence of T_C on x (open symbols in figure 2(a)) with predictions of the Varma model for the A samples (dotted line in figure 2(a)) is obtained for $W = 1.90$ eV and $\delta = 0.071$. The function $c(x)$ evaluated for the A samples with equation (3) (dotted line in figure 2(b)) lies slightly above that of the B samples. Hence,

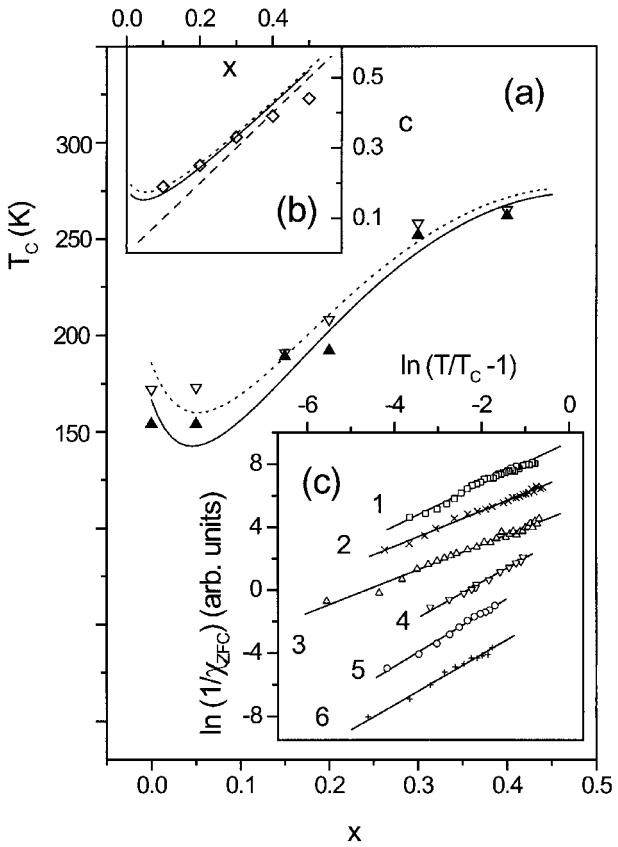

Figure 2. (a) Dependence of T_C on x for A samples (open triangles, [23]) and for B samples (closed triangles, this work) and the fits with equation (1) (dotted line from [23] and solid line from this work). (b) Dependence of c on x evaluated with equation (3) for the A samples (dotted line, [23]), for the B samples (solid line, this work) and the data from [3] (open symbols). The dashed line represents the concentration of Ca^{2+}, $c = x$. (c) Critical behaviour of χ_{ZFC} near the Curie temperature for samples 1–6.

the results of the analysis of $T_C(x)$ for our LCMO samples correlate well with each other and with published data [3]. The high-temperature annealing leads to a small decrease of the concentration of the Mn^{4+} ions (cf tables 1 and 2) via some diminution of the effective parameter δ.

Finally, we determine the critical exponent, γ, of the temperature dependence of the inverse susceptibility near the FM to PM transition ($T > T_C$),

$$\chi^{-1}(T) \propto \left(\frac{T}{T_C} - 1\right)^{\gamma}. \tag{4}$$

The plots of $\ln(1/\chi_{ZFC})$ against $\ln(T/T_C - 1)$ shown in figure 2(c) for the B samples 1–6 demonstrate a critical behaviour for all specimens and can be fitted well with a linear function. The values of γ are given as a function of x in figure 3(a) and as a function of c in figure 3(b). In these figures are displayed also the values of γ obtained from the critical behaviour of χ in the A samples [23]. For both A and B samples the results are quite different in the intervals of $0 \leqslant x < 0.18$ ($0.15 \leqslant c < 0.23$) where $\gamma = 1.20 \pm 0.05$ and $0.18 < x \leqslant 0.4$ ($0.23 < c \leqslant 0.43$) where $\gamma^* = 1.64 \pm 0.06$.

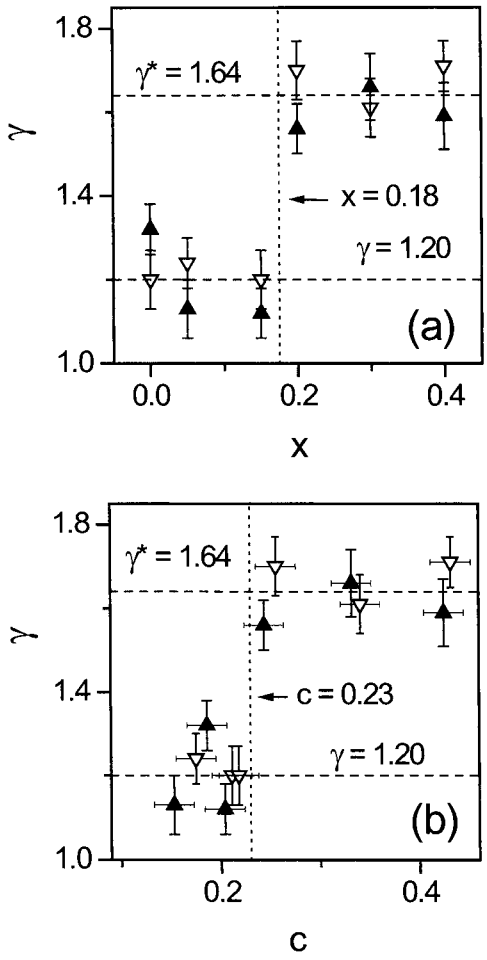

Figure 3. The critical exponent γ plotted for different x (a) and for corresponding values of c (b). The closed symbols represent the data obtained for the A samples [23] and the open symbols for the B samples (this work).

The values of γ lie between predictions of the 3D Heisenberg model ($\gamma = 1.4$) and the mean-field theory ($\gamma = 1$) [24]. Similar values of γ have been found in $La_{0.67}(Ba_yCa_{1-y})_{0.33}MnO_3$ ($\gamma = 1.29$, 1.11 and 1.12 for $y = 1$, 0.5 and 0.25, respectively) from analysis of modified Arrot plots [25]. A lower value, $\gamma = 1.08$, was obtained in $La_{0.8}Sr_{0.2}MnO_3$ [26], while those close to the 3D Heisenberg model were found in $La_{1-x}Sr_xCoO_3$ ($\gamma = 1.39$ for $x = 0.20$ and 0.25 and 1.43 for $x = 0.30$) [27].

The values of γ^* are similar to those calculated numerically in the percolation theory for the 3D case: $\gamma_p = 1.69 \pm 0.05$ [28] and 1.70 ± 0.11 [29]. On the other hand, additional investigations are required to ensure that γ^* found above for LCMO with $x > 0.18$ and $c > 0.23$ really represents the critical exponent. The point is that by the analysis of the Arrot plots in $La_{0.67}(Ba_yCa_{1-y})_{0.33}MnO_3$ it was established that only in the samples with $y \geqslant 0.25$ the magnetic properties follow the behaviour expected for a conventional second-order FM transition [25]. Comparative investigations of the PM to FM transition in $La_{0.7}Ca_{0.3}MnO_3$ and $La_{0.7}Sr_{0.3}MnO_3$ [30, 31] led the authors to conclude that the phase transition changes from the

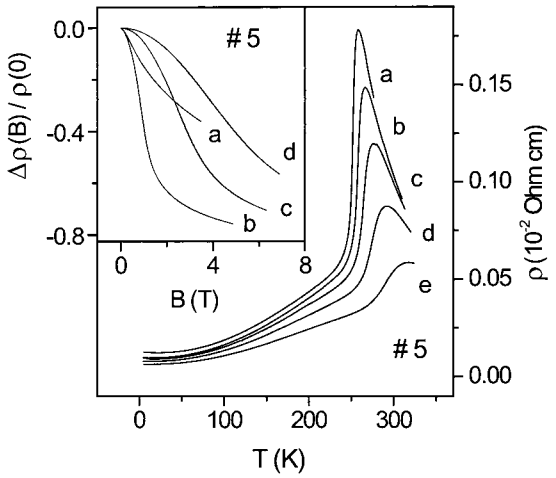

Figure 4. Dependence of the resistivity on temperature observed in sample 5 ($x = 0.3$) for $B = 0$ (line a), 1 T (line b), 2 T (line c), 4 T (line d) and 8 T (line e). Inset: dependence of the relative magnetoresistance on the magnetic field for $T = 244$ K (line a), 258 K (line b), 273 K (line c) and 290 K (line d).

second to the first order when Ca is substituted for Sr. Additionally, in $La_{0.7-y}Pr_yCa_{0.3}MnO_3$ a hysteresis of the temperature dependence of the resistivity, $\rho(T)$, observed near T_C for the compositions with $y = 0.175$–0.6 demonstrates that in these samples the FM transition is of the first order [32]. However, no hysteresis of $\rho(T)$ can be seen in this compound at $y = 0$ [33]. In LCMO with $0.125 \leqslant x \leqslant 0.5$, the hysteresis of $\rho(T)$ was found only for $x = 0.5$ [34], what is a typical feature of the charge-ordered state. In figure 4 are presented the temperature dependences of the resistivity, $\rho(T)$ of our sample 5 with $x = 0.3$ in fields $B = 0$, 1, 2, 4 and 8 T, and in the inset of figure 4 the relative magnetoresistance (MR) of the same sample for $T = 244$, 258, 273 and 290 K. The DC measurements performed with the standard four probe method yielded no difference between $\rho(T)$ measured by increasing and decreasing T at any applied field or in any temperature interval between $T = 5$ and 320 K. The absence of the temperature hysteresis near T_C suggests that the phase transition in this specimen is not of the first order.

3.2. Magnetic irreversibility and ageing phenomena in LCMO

In this subsection we discuss the irreversibility of the magnetic susceptibility (figure 1) and results in long-time relaxation of TRM in LCMO. In frustrated systems the deviation between $\chi_{ZFC}(T)$ from $\chi_{FC}(T)$ is governed by spin dynamics and is usually observed below the onset of freezing-in of the magnetic moments. In LCMO the frustration may be a consequence of (i) the presence of disorder in stacking of Mn^{3+} and Mn^{4+} ions for $c < c^*$ ($c^* \approx 0.5$ is the concentration at which the charge ordered state is observed) accompanied by competing SE–DE interactions [35] and (ii) phase separation or existence of randomly distributed hole-rich droplets (nanometre size magnetic polarons or clusters) with interactions different from the lattice [15–18].

We assume that in LCMO the cusp of $\chi_{ZFC}(T)$ at T_f may be governed by local anisotropy fields acting on the magnetic moments. The spins may be frozen in directions energetically favoured by their local anisotropy or by the external field if the system is cooled

down from $T > T_f$ in zero or nonzero field, respectively, leading to a difference between $\chi_{ZFC}(T)$ and $\chi_{FC}(T)$. In this case there would be a competition between the local anisotropy and the influence of the external field. The former is predominant for $T < T_f$ and the latter for $T > T_f$. Therefore, we suppose that the cusp of $\chi_{ZFC}(T)$ marks a crossover region where the average anisotropy energy and the energy caused by the external field are comparable.

In figures 5(a) and (b) are shown the temperature dependences of TRM$/B$ (closed triangles) for the samples 1–5 and in figure 5(c) for the samples 1^*, 2^* and 5^*. They are compared with the differences $\chi_{FC}(T) - \chi_{ZFC}(T)$ (open triangles) obtained for the same specimens. In SGs a coincidence of the functions TRM(T) and $M_{FC}(T) - M_{ZFC}(T)$ may be expected [36]. In CGs deviations from this behaviour may arise due to anisotropy of the clusters, possibly associated with their shape and orientation [36].

As evident from figures 5(a) and (b) there is a perfect coincidence of TRM(T) and $M_{FC}(T) - M_{ZFC}(T)$ for samples 1 and 2 ($x = 0$ and 0.05, respectively), whereas for samples 3–5 ($x = 0.15$–0.3) distinct deviations are observed. A better coincidence between TRM(T) and $M_{FC}(T) - M_{ZFC}(T)$ for smaller $x = 0$ and 0.05 (1^* and 2^*, respectively) is changed to a clear deviation for $x = 0.3$ (5^*) also in the A samples (figure 5(c)). Quite similar behaviour of TRM(T) and $M_{FC}(T) - M_{ZFC}(T)$ has been found in CoAlT (T is a transition-metal element) [37] and in CoGa [36] systems when a transition from SG to CG is induced by doping or by non-stoichiometry. In these systems the equation

$$M_{FC}(T, B) - \mathrm{TRM}(T) = M_{ZFC}(T) - 0 \tag{5}$$

was attributed to the symmetry of the energy distribution of potential barriers in the SG with respect to the presence or absence of a magnetic field (0 represents the zero level of the magnetization). When the system is heated it can make a transition to that metastable state which is separated by an energy barrier not exceeding the thermal activation energy expressed by the $M_{ZFC}(T) - 0$ value. When the field is switched on the SG adopts a certain metastable state $M_{FC}(T, B)$ depending on the temperature and the field. After switching off the field the system reflects the TRM(T). Finally, comparison between TRM(T) and $M_{FC}(T) - M_{ZFC}(T)$ of LCMO at different x for both groups of specimens is consistent with a transition from SG to CG when x is increased, where SG is probably due to the first while CG to the second of the two possible reasons for frustration in LCMO mentioned above.

In figure 6(a) is shown the relaxation of TRM observed over a time scale of 10^4 s for the samples 1^*, 2^* and 3^* after the wait times $t_W = 1.8$, 3.4 and 3.5×10^3 s, respectively, plotted together with the relaxation rate, $S(t) = -\mathrm{d}\,\mathrm{TRM}(t)/\mathrm{d}\log t$. A systematic change of the curvature of the relaxation curves of TRM(t) from concave-down to concave-up can be seen with increasing t, with an inflection point visible also as a maximum of the function $S(t)$ near t_W. The corresponding data for samples 2 (for $t_W = 3.6 \times 10^3$ and 1.1×10^4 s) and 5 (for $t_W \approx 10^3$ s) are displayed in figures 6(b) and (c), respectively. A well observable shift of the maximum of $S(t)$ when t_W is increased (figure 6(b)) should also be mentioned. Additionally, one can see also distinct differences between the samples 2 and 5, e.g. nearly one order of magnitude drop of $S(t)$ when x is increased from 0.05 to 0.2 (figure 6(c)). In more detail the evolution of the relaxation rate with increasing x, plotted for different temperatures for the observation time $t = 10^3$ s (which is chosen near the maximum of $S(t)$ at $t_W = (2$–$5) \times 10^3$ s) is shown in figure 7. The clear maximum of the function $S(T)$ evident for all specimens in figure 7 results from the competition between two processes, freezing of the magnetic moments when T is decreased and activation of the frozen-in moments with increasing T. Therefore, this maximum corresponds to the freezing temperature T_f also, while the long-time relaxation is observed not only below but also above T_f.

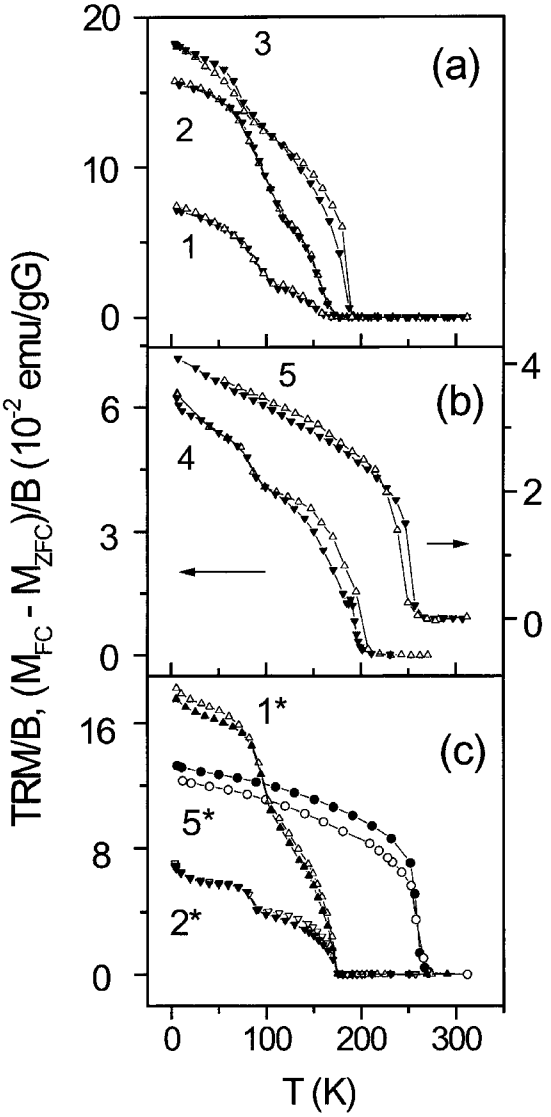

Figure 5. Temperature dependence of TRM/B (closed symbols) and $(M_{FC} - M_{ZFC})/B$ (open symbols) for the samples 1–5 (a), (b) and for the samples 1*, 2* and 5* (c).

Ageing effects closely similar to those in figure 6 are often observed in an SG, CG or in the FM phase of a reentrant spin-glass [38]. They reflect the non-equilibrium character of frustrated systems. The long-time relaxation phenomena observed in LCMO evidences an important role of frustration in this system. However, its origin is non-universal in LCMO in the different intervals of the composition. As seen from figure 7, for $x = 0$–0.15 the plots of $S(T)$ collapse into one curve below $\approx$80 K. This does not take place for samples 4* and 5* with larger values of x. This suggests a different origin of the glassy state for the two different intervals of the composition, $x \leqslant 0.15$ and $x \geqslant 0.2$, respectively.

Next we analyse the functions TRM(t) for samples 2 and 5 with $x = 0.05$ and 0.2, respectively, chosen from each of the two intervals of the composition mentioned above, with

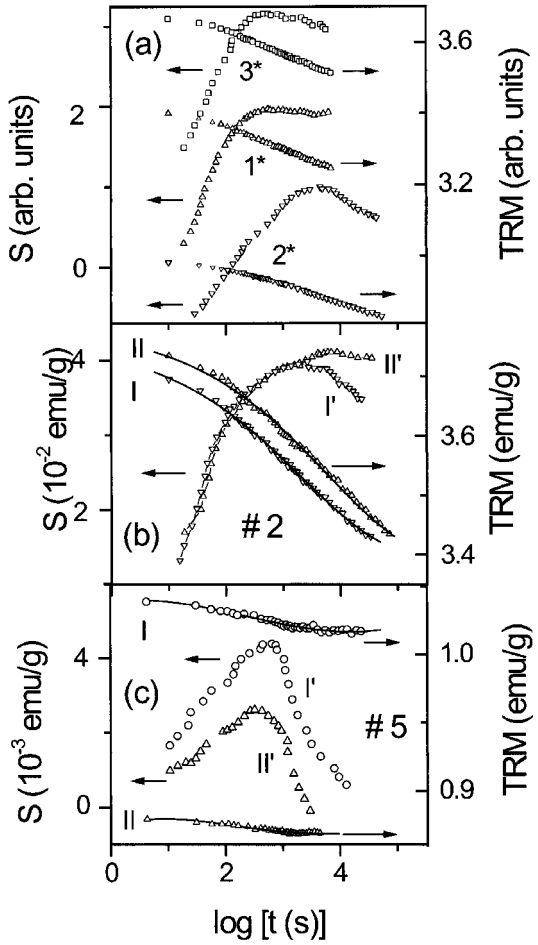

Figure 6. Dependences of TRM and S on $\log t$ (a) for the samples 1* at 80 K, 2* at 65 K and 3* at 75 K, measured after a wait time of $t_W = 1.8 \times 10^3$, 3.4×10^3 and 3.5×10^3 s, respectively, (b) for sample 2 at 90 K after $t_W = 3.6 \times 10^3$ s (I, I′) and 1.1×10^4 s (II, II′) and (c) for sample 5 at 200 K (I, I′) and 240 K (II, II′) after $t_W \approx 10^3$ s.

the stretched exponential law. The form

$$M(t) = M_0 + M_1 \exp[-(t/\tau)^{1-n}] \tag{6}$$

where the parameters M_0, M_1 and the response time τ do not depend on the observation time (but may depend on the temperature and t_W) and n is a constant, is often used as a good approximation of long-time relaxation in SGs when t_W is comparable with the observation time [39–41]. All the TRM(t) curves for samples 2 and 5 can be fitted well with equation (6) (the solid lines in figure 6). An equal value of $n = 0.65 \pm 0.12$ is observed for both specimens. It does not vary systematically with temperature and is independent of t_W. The value of n is equal to that found in the metallic spin glass AgMn ($n = 0.65$) [39] and similar to those in CoAlCu ($n = 0.77$–0.79) [40] and in the CG region of CrFe ($n = 0.49$–0.74, depending on t_W), but is lower than in the re-entrant FM region of this compound ($n = 0.88$–0.92) [41]. The response time τ for sample 2 is found to be sensitive to t_W, $\tau = 2.1 \times 10^3$ and 5.2×10^3 s for $t_W = 3.6 \times 10^3$ and 1.1×10^4 s, respectively. The parameters τ, M_0 and M_1 versus T are

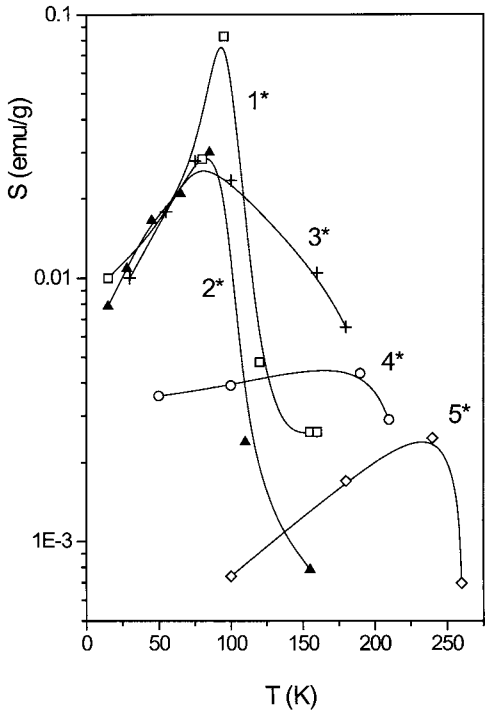

Figure 7. Dependence of the relaxation rate S on T at $t = 10^3$ s for the samples 1*–5*. The solid lines are guides for the eye.

displayed in figures 8(a), (b) and (c). Their temperature dependence is quite different for the samples 2 (open triangles) and 5 (closed triangles). The dependence of τ for 2 is very strong and can be characterized by an exponential function, similar to that of AgMn [38], while for 5 τ does not exhibit a systematic variation with T (figure 8(a)). The dependence of M_0 on T is nearly linear and is also much stronger in 2 than in 5. The function $M_1(T)$ in sample 2 decays nearly exponentially while in sample 5 it does not depend on T. These drastic differences of the ageing effects in these two samples with different compositions support the conjecture that in LCMO the SG state at low x transforms into the CG state when x is increased.

4. Summary and conclusions

Low-field magnetic properties of LCMO, including samples subjected to an additional high-temperature heat treatment at 1520 °C, are investigated. All samples demonstrate a PM to FM transition. The dependence of the transition temperature, T_C, on the concentration of Mn^{4+} ions is analysed with the model of Varma [14], considering spin polarons associated with electronic localization and electron–electron interactions. The dependence of the concentration of Mn^{4+} ions on x is obtained by taking into account the formation of vacancies in the cation sublattice. At low x the values of c deviate distinctly from the concentration of Ca^{2+} and agree with those found in [3]. The bandwidth of the localized electrons, $W = 1.88 \pm 0.06$ eV, is found to be similar to that in $La_{1-x}Sr_xMnO_3$ (2.5 eV) [14] and is independent of the final annealing temperature of the samples (1.9 eV) [23]. It is shown also that the high-temperature annealing leads to some decrease of the Curie temperature and to a small decrease of the

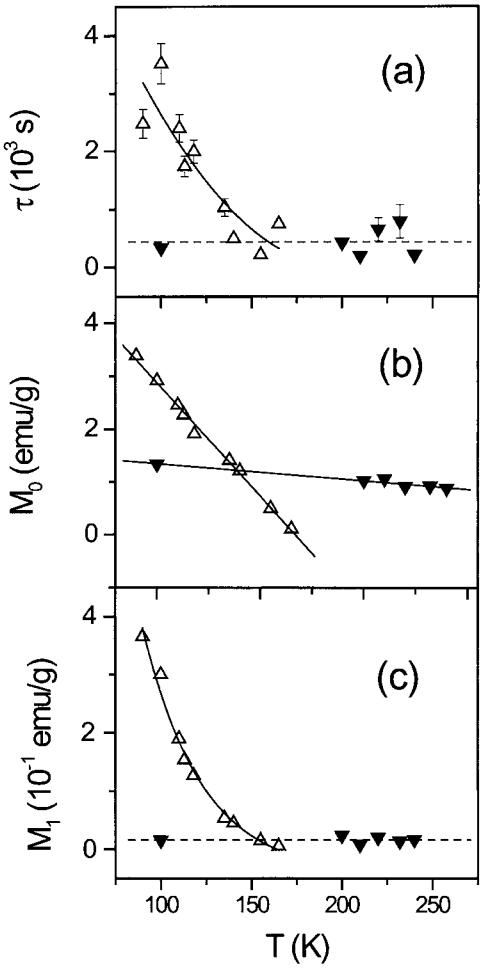

Figure 8. Temperature dependences of τ (a), M_0 (b) and M_1 (c) for LCMO with $x = 0.05$ (sample 2, open symbols) and 0.30 (sample 5, closed symbols). The solid lines are guides for the eye.

concentration of Mn^{4+} ions due to diminution of the effective concentration of the cation vacancies.

$\chi_{ZFC}(T)$ exhibits critical behaviour near T_C in all the investigated samples. For $x < x_b$ ($c < c_b$), where $x_b \approx 0.18$ and $c_b \approx 0.23$, the value of the critical exponent $\gamma = 1.20 \pm 0.05$ lies between those of the mean-field theory ($\gamma = 1$) and of the 3D Heisenberg model ($\gamma = 1.4$). Values of γ between these two limits have been obtained from modified Arrot plots for $La_{0.67}(Ba_yCa_{1-y})_{0.33}MnO_3$ with $y \geqslant 0.25$ [25]. For $x > x_b$ ($c > c_b$) our value of $\gamma^* = 1.64 \pm 0.06$ is close to $\gamma_p = 1.69 \pm 0.05$ [28] and 1.70 ± 0.11 [29], calculated in the percolation theory.

It is worth noting that in some manganite perovskite systems the FM transition may be of the first order [25, 30–32]. In this case x_b or c_b would be upper limits of the corresponding concentrations where the PM to FM transition in LCMO is still of second order. On the other hand, no traces of temperature hysteresis is observed in our sample with $x > x_b$ and $c > c_b$ (sample 5), in contradiction to the conjecture about the first-order phase transition.

The irreversibility of the magnetic susceptibility of LCMO starting close to T_C implies that LCMO does not represent below the PM to FM transition a true magnetically ordered state at any x between 0 and 0.4. Additionally, the cusp at T_f in $\chi_{ZFC}(T)$ for the samples with $x = 0$ and 0.05 is changed to a rounded maximum at $x = 0.3$, while the relative deviation of $\chi_{ZFC}(T)$ from $\chi_{FC}(T)$ is diminished. The difference $\chi_{FC}(T) - \chi_{ZFC}(T)$ coincides with the $\mathrm{TRM}(T)/B$ curve for $x \leqslant 0.05$ but deviates from this behaviour when x is increased.

Long-time relaxation of TRM observed over a time scale of 10^4 s is reported for the first time in LCMO. The relaxation rate $S(t)$ attains a maximum near t_W. This maximum is shifted when t_W is increased. Additionally, the function $S(T)$ reaches a maximum near the freezing temperature. The behaviour of $S(T)$ is different for the samples with $x \leqslant 0.15$ and $\geqslant 0.2$. The time relaxation of TRM can be well described with a stretched exponential law. However, the temperature dependences of the effective parameters M_0, M_1 and the response time τ entering this law are quite different for the samples with $x = 0.05$ and 0.3. These features reflect an important role of the frustration in the magnetic state of LCMO at any x between 0 and 0.4 and are consistent with the transformation of the SG state at low x to the CG state when x is increased. The SG may be connected with the lattice disorder and competing SE–DE interactions [35], while the CG is probably due to phase separation and existence of hole-rich regions (nanoclusters or magnetic polarons) with properties and interactions different from the main material [15–18].

References

[1] von Helmolt R, Wecker J, Holzapfel B, Schulz L and Sammer K 1993 *Phys. Rev. Lett.* **71** 2331
[2] Wollan E O and Koehler W C 1955 *Phys. Rev.* **100** 545
[3] Mahendrian R, Tiwary S K, Raychaudhuri A K, Ramakrishnan T V, Mahesh R, Rangavittal N and Rao C N R 1996 *Phys. Rev.* B **53** 3348
[4] de Brion S, Ciorcas F, Chouteau G, Lejay P, Radaelli R and Chaillout C 1999 *Phys. Rev.* B **59** 1304
[5] Töpfer J and Goodenough J B J 1997 *Solid State Chem.* **130** 117
[6] Schiffer P, Ramirez A P, Bao W and Cheong S-W 1995 *Phys. Rev. Lett.* **75** 3336
[7] Chen C H and Cheong S-W 1996 *Phys. Rev. Lett.* **76** 4042
[8] Roy M, Mitchell J F, Ramirez A P and Schiffer P 1999 *J. Phys.: Condens. Matter* **11** 4843
[9] Zener C 1951 *Phys. Rev.* **82** 403
[10] de Gennes P-G 1960 *Phys. Rev.* **118** 141
[11] Millis A J, Littlewood P B and Shairman B I 1995 *Phys. Rev. Lett.* **74** 5144
[12] Röder H, Zang J and Bishop R 1996 *Phys. Rev. Lett.* **76** 1356
[13] Millis A J, Shairman B J and Mueller R 1996 *Phys. Rev. Lett.* **76** 1356
[14] Varma C M 1996 *Phys. Rev.* B **54** 7328
[15] Hennion M, Moussa F, Biotteau G, Rodriguez-Carvajal J, Piusard L and Revcolevschi A 1998 *Phys. Rev. Lett.* **81** 1957
[16] Lynn J W, Ervin R W, Borchers J A, Huang Q, Santoro A, Peng J-L and Li Z Y 1996 *Phys. Rev. Lett.* **76** 4046
[17] Pissas M, Kallias G, Devlin E, Simopoulos A and Niarchos D 1997 *J. Appl. Phys.* **81** 5770
[18] Chechersky V, Nath A, Isaac I, Franck J P, Ghosh K, Ju H and Greene R L 1999 *Phys. Rev.* B **59** 497
[19] Li X-G, Fan X J, Ji G, Wu W B, Wong K H, Choy C L and Ku H C 1999 *J. Appl. Phys.* **85** 1663
[20] Itoh M, Natori I, Kubota S and Motoya K 1994 *J. Phys. Soc. Japan* **63** 1486
[21] Gayathni N, Raychandhuri A K, Tiwary S K, Gundakaram G, Arulraj A and Rao C N R 1997 *Phys. Rev.* B **56** 1345
[22] Nam D N H, Jonason K, Nordblad P, Khiem N V and Phuc N X 1999 *Phys. Rev.* B **59** 4189
[23] Laiho R, Lisunov K G, Lähderanta E, Petrenko P A, Stamov V N and Zakhvalinskii V S 2000 *J. Magn. Magn. Mater.* **213** 271
[24] Stanley H E 1971 *Introduction to Phase Transitions and Critical Phenomena* (Oxford: Clarendon)
[25] Moutis N, Panagiotopulos I, Pissas M and Niarchos D 1999 *Phys. Rev.* B **59** 1129
[26] Mohan Ch V, Seeger M, Kronmuller H, Murugaraj P and Maier J 1998 *J. Magn. Magn. Mater.* **183** 348
[27] Mira J, Rivas J, Vazques M, Garcia-Beneyetz J M, Arcas J, Sanchez R D and Senaris-Rodriguez M A 1999 *Phys. Rev.* B **59** 123

[28] Sykes M F and Essam J W 1964 *Phys. Rev.* **133** 310
[29] Dunn AG, Essam J W and Ritchie D S 1975 *J. Phys. C: Solid State Phys.* **8** 4219
[30] Mira J, Rivas J, Rivadulla F, Vazquez-Vazquez C and Lopez-Quintela M A 1999 *Phys. Rev.* B **60** 2998
[31] Novak P, Marysko M, Savosta M M and Ulyanov A N 1999 *Phys. Rev.* B **60** 6655
[32] Hwang H Y, Cheong S-W, Radaelli P G, Marezio M and Batlogg B 1995 *Phys. Rev. Lett.* **75** 914
[33] Hiroto K, Kaneto N, Nishizawa A and Endo E 1996 *J. Phys. Soc. Japan* **65** 3736
[34] Dlo J, Kim I, Lee S, Kim K H, Lee H J, Jung J H and Noh T W 1999 *Phys. Rev.* B **59** 492
[35] de Almeida J R L 1999 *J. Phys.: Condens. Matter* **11** L 223
[36] Belous N, Zorin I, Kulich N, Lezhnenko I and Tovstolytkin A 1990 *Sov. Phys.–Solid State* **32** 887
[37] Lähderanta E, Eftimova K, Laiho R, Kanani H Al and Booth J G 1994 *J. Magn. Magn. Mater.* **130** 23
[38] Jonason K, Mattson J and Nordblad P 1996 *Phys. Rev.* B **53** 6507
[39] Hoogerbeets R, Luo Wei-Li and Orbach R 1986 *Phys. Rev.* B **34** 1719
[40] Lähderanta E, Eftimova K and Laiho R 1995 *J. Magn. Magn. Mater.* **139** 18
[41] Mitchler P, Roshko R M and Ruan W 1993 *J. Appl. Phys.* **73** 5460